Carbohydrate Polymers 92 (2013) 1451–1462

Contents lists available at SciVerse ScienceDirect

Carbohydrate Polymers

journal homepage: www.elsevier.com/locate/carbpol

Molecular and supra-molecular structure of waxy starches developed from cassava (*Manihot esculenta* Crantz)

Agnès Rolland-Sabaté[a,*], Teresa Sanchez[b], Alain Buléon[a], Paul Colonna[a], Hernan Ceballos[b], Shan-Shan Zhao[c], Peng Zhang[c,d], Dominique Dufour[b,e,f]

[a] *UR1268 Biopolymères Interactions Assemblages, INRA, F-44300 Nantes, France*
[b] *Centro Internacional de Agricultura Tropical (CIAT), A. A. 6713, Cali, Colombia*
[c] *National Key Laboratory of Plant Molecular Genetics, Institute of Plant Physiology and Ecology, Shanghai Institutes for Biological Sciences, Chinese Academy of Sciences, 300 Fenglin Road, Shanghai 200032, China*
[d] *Shanghai Chenshan Plant Science Research Center, Chinese Academy of Sciences, Shanghai Chenshan Botanical Garden, 3888 Chenhua Road, Shanghai 201602, China*
[e] *Centre de Coopération Internationale en Recherche Agronomique pour le Développement (CIRAD), UMR QUALISUD, 34398 Montpellier, France*
[f] *CIRAD-UMR QUALISUD, Cali, Colombia*

ARTICLE INFO

Article history:
Received 30 July 2012
Received in revised form 12 October 2012
Accepted 19 October 2012
Available online 27 October 2012

Keywords:
Amylopectin
Waxy
Genetic variation
Structural characterization
Cassava

ABSTRACT

The aim of this work was to characterize the amylopectin of low amylose content cassava starches obtained from transgenesis comparatively with a natural waxy cassava starch (WXN) discovered recently in CIAT (International Center for Tropical Agriculture). Macromolecular features, starch granule morphology, crystallinity and thermal properties of these starches were determined. $\bar{M}_w$ of amylopectin from the transgenic varieties are lower than WXN. Branched and debranched chain distributions analyses revealed slight differences in the branching degree and structure of these amylopectins, principally on DP 6–9 and DP > 37. For the first time, a deep structural characterization of a series of transgenic lines of waxy cassava was carried out and the link between structural features and the mutated gene expression approached. The transgenesis allows to silenced partially or totally the GBSSI, without changing deeply the starch granule ultrastructure and allows to produce clones with similar amylopectin as parental cassava clone.

1. Introduction

Starch is the principal energy reserve in plants and is one of the most abundant carbohydrates in the biosphere. Starch in storage organs (kernels, roots, tubers or stems) from different crops is the most important energy source for human and animal consumption as well (Blennow, 2000). Man has extended the use of starch far beyond its role as source of energy (adhesives, agrochemicals, cosmetics, detergents, medical oil and gas, paper and board, pharmaceutical, plastics, purification, beverages, textile, etc.). Many different *in vitro* chemical, physical or biochemical modifications (cross-linking, stabilization, dextrinization, enzyme conversions, oxidation lipophilic substitution, pregelatinization, thermal treatments) enable the evolution of new processing technologies and market trends (BeMiller, 1997; Jobling, 2003; Taggart, 2000). However, many of these modifications are expensive and environmentally unfriendly. There is also an increasing consumer's preference for more "natural" products. These factors explain the growing interest of achieving these modifications *in planta* (Davis, Supatcharee, Khandelwal, & Chibbar, 2003; Ellis et al., 1998; Zeeman, Kossmann, & Smith, 2010).

Corn starch is the most widely used as a food ingredient, and its chemical derivatives have extended the range of functional properties available. Cassava (*Manihot esculenta* Crantz) is particularly important as a source of starch in tropical and subtropical regions of the world. In fact, no other source of starch is traded more in the international markets than that of cassava (Stapleton, 2012). Tropical root and tuber crops may be crucial as subsidiary or subsistence food crops in different parts of the tropical belt. Also, when processed into starch, they result in rural development and poverty alleviation. Starch from cassava produces relatively bland pastes, with higher viscosity, better clarity and lower retrogradation rates than starches from cereals. They also possess lower levels of proteins and lipids (Davis et al., 2003; Ellis et al., 1998; Sánchez et al., 2009). Two natural cassava starch mutations have been reported recently (Ceballos et al., 2007, 2008). In addition, transgenic waxy cassavas have been described (Koehorst-van Putten et al., 2012;

* Corresponding author at: Unité de Recherche sur les Biopolymères, Interactions et Assemblages, INRA, BP 71627, 44316 Nantes Cedex 03, France.
Tel.: +33 0 240 67 51 48; fax: +33 0 240 67 51 67.
E-mail addresses: sabate@nantes.inra.fr (A. Rolland-Sabaté), t.sanchez@cgiar.org (T. Sanchez), Alain.Buleon@nantes.inra.fr (A. Buléon), Paul.Colonna@nantes.inra.fr (P. Colonna), h.ceballos@cgiar.org (H. Ceballos), zhangpeng@sibs.ac.cn (P. Zhang), d.dufour@cgiar.org (D. Dufour).

0144-8617/$ – see front matter © 2012 Elsevier Ltd. All rights reserved.
http://dx.doi.org/10.1016/j.carbpol.2012.10.048

List of symbols

$\bar{B}$	average number of branching points in the ABC three-functional polycondensation model
$\bar{B}_{mH}$	average number of branching points obtained using theoretical amylopectin structures as proposed by Hizukuri (1986)
BD	branching degree
BD_{mH}	branching degree obtained using theoretical amylopectin structures as proposed by Hizukuri (1986)
$\overline{CL}$	average chain length
d_{Gappw}	apparent particle density calculated on the basis of a smeared uniform density in the particle using the following equation: $d_{Gappw} = \bar{M}_w/(4\pi/3)\bar{R}^3_{GW}$
DP	degree of polymerization
$\overline{DP}_w$	weight average degree of polymerization
$\overline{DP}_w/\bar{B}$	average number of glucosyl units in a linear chain per branching point
$\overline{DP}_w/\bar{B}_{mH}$	average number of glucosyl units in a linear chain per branching point obtained using theoretical amylopectin structures as proposed by Hizukuri (1986)
ΔH	gelatinization enthalpy
DSC	differential scanning calorimetry
g_M	average shrinking factor or average branching parameter
IBC	iodine binding capacity
K_G	constant
λ_{max}	wavelength at maximum absorption of the iodine complexes with starch polymers
M	molar mass of a fraction
$\bar{M}_n$	number average molar mass
$\bar{M}_w$	weight average molar mass
$\bar{M}_w/\bar{M}_n$	dispersity index
ν_G	hydrodynamic coefficient
R_G	radius of gyration of a fraction
$\bar{R}_{GW}$	weight average radius of gyration
$\bar{R}_{GW(br)}$	weight average radius of gyration of the branched polymer
$\bar{R}_{GW(lin)}$	weight average radius of gyration for the corresponding linear polymer
$\bar{R}_{Gz}$	z-average radius of gyration
R_H	hydrodynamic radius
T_c	conclusion temperature
T_o	onset temperature gelatinization
T_p	peak temperature gelatinization

Zhao, Ceballos, Dufour, Sánchez, & Zhang, 2011). New botanical sources thus need to be investigated and it is worth focusing on tropical sources because of their special functional properties and social and economic relevance.

The present work thus aimed to characterize the amylopectin of low amylose content cassava starches obtained from transgenesis and compare them with a natural waxy cassava starch discovered recently (Ceballos et al., 2007). An important output of this work would be to point out the structural differences between the natural and transgenic cassava clones and to relate these structural differences to the mutated genes.

2. Materials and methods

2.1. Materials

Eight starches from different cassava genotypes were studied. The natural waxy cassava (WXN), identified from a self-pollinated generation, and its roots were obtained at CIAT (Centro Internacional de Agricultura Tropical, Colombia) using the procedures previously described (Ceballos et al., 2007). The transgenic expected waxy cassava plants were produced by the SIBS-ETH Shanghai Center for Cassava Biotechnology (Shanghai Institutes for Biological Sciences, China) from the West African cassava cultivar TMS 60444 (TMS60444) using the procedures previously described (Zhang, Potrykus, & Puonti-Kaerlas, 2000; Zhao et al., 2011). They were cultivated in greenhouse controlled conditions. The transgenic clones, produced using p54/1.0::GBSSI-RNAi, were named A clones, and those produced using 35S::GBSSI-RNAi were named B lines. After phenotypic screening, 6 plant lines with normal growth and development were chosen for this study (A19, B8, B9, B10, B13 and B23). The starches from these six potentially waxy genotypes, as well as that from the original TMS60444 non-waxy genotype were isolated according to the procedure described by Ceballos et al. (2007). Isoamylase from Pseudomonas amyloderamosa (glycogen 6-glucanohydrolase; EC 3.2.1.68) with an activity of 59,000 U mL^{-1} was from Hayashibara Shoji Inc. (Okayama, Japan).

2.2. Methods

2.2.1. Determination of amylose content

Amylose content was determined by three different approaches: colorimetry (standard ISO6647 procedure, as described in Pérez et al., 2011), differential scanning calorimetry (DSC) (Ceballos et al., 2007, 2008) and quantification of iodine binding capacity (IBC) (Pérez et al., 2011). The wavelength at maximum absorption of the iodine complexes (λ_{max}) was determined as previously described (Rolland-Sabaté, Colonna, Potocki-Véronèse, Monsan, & Planchot, 2004).

2.2.2. Structure and properties of the starch granule

The morphology of the native granules was observed using scanning electron microscopy (SEM). The granules were deposited onto copper stubs and allowed to dry. The specimens were coated with Au–Pd, examined at 10.0 kV, and imaged using a JEOL JSM 5800LV scanning electron microscope. Crystallinity information and starch granule sizes were determined as previously described (Pérez et al., 2011).

Gelatinization temperature and enthalpy were analyzed by DSC using a TA Instruments DSC Q100 device (TA Instruments, Norwalk, CT, USA) with sealed stainless steel pans as previously described (Rolland-Sabaté et al., 2012). Gelatinization onset temperature (T_o), gelatinization peak temperature (T_p) and gelatinization enthalpy (ΔH), of each sample were then determined from the thermograms using the Universal Analysis (TA Instruments) software and normalized to the mass of dry matter. The moisture content was determined by thermogravimetric analysis at a heating rate of 10 °C min^{-1} until 130 °C and then 130 °C for 20 min.

Mild acid hydrolysis by HCl (lintnerization) was used as a means to study the ultrastructure of the starch granule. The native starch granule was lintnerized as previously described (Gérard, Colonna, Buléon, & Planchot, 2002) and the amount of solubilized product was quantified using the sulfuric acid–orcinol colorimetric method (Planchot, Colonna, & Saulnier, 1997). The extent of hydrolysis was expressed as the percentage of dry substrate solubilized. The crystallinity of lintnerized starch granules was determined using X-ray diffraction and their morphology observed by SEM. The chain distribution of lintnerized samples was determined using high-performance anion-exchange chromatography with pulsed amperometric detection (HPAEC-PAD) (Model DX-120, Dionex, Sunnyvale, CA, USA), using Carbopac PA100 (4 mm × 250 mm) column, as previously described (Rolland-Sabaté et al., 2012). The degree of polymerization (DP) of individual peaks were identified

by using a series of maltooligosaccharide standards of DP between 2 and 7. It should be noticed that as in HPAEC-PAD response coefficients decrease with increasing DP, % area of long chains are not representative of the exact weight fraction of each DP.

2.2.3. Macromolecular characteristics

Molar mass, size, conformation and branching were obtained using asymmetrical flow field flow fractionation (A4F) coupled with multi-angle laser light scattering (MALLS) using the same procedure and set up as described by Rolland-Sabaté et al. (2012).

The samples were first dissolved in a DMSO/water (95/5) mixture and then solubilized in water by microwave heating under pressure (Rolland-Sabaté, Colonna, Mendez-Montealvo, & Planchot, 2007). Solutions were filtrated through 5 μm Durapore™ membranes (Waters, Bedford, MA, USA) and immediately injected into the A4F-MALLS-QELS system. A4F equipment, including the asymmetrical channel, Control-Box V3, Flow box P2.1 and the valve box, was obtained from Consenxus (Ober-Hilbersheim, Germany). The device, its configuration, the membrane and the flow method for A4F fractionation were exactly the same as previously described (Rolland-Sabaté et al., 2007).

The dual detection of solutes was carried out using a Dawn® Heleos™ MALLS system fitted with a K5 flow cell and a GaAs laser, (λ = 658 nm), supplied by Wyatt Technology Corporation (Santa Barbara, CA, USA) and an ERC-7515A refractometer from Erma (Tokyo, Japan). Before use, the mobile phase (Millipore water containing 0.2 g L^{-1} sodium azide) was carefully degassed and filtered through Durapore GV (0.2 μm) membranes from Millipore, and eluted at a flow rate of 1 mL min^{-1}. Solubilization recoveries were calculated from the ratio of the initial mass and the mass after filtration, and elution recoveries from the ratio of the mass eluted from the A4F channel (integration of the differential refractive index (DRI) signal) and the mass injected. Carbohydrate concentrations were determined using the sulfuric acid–orcinol colorimetric method (Planchot et al., 1997).

$\bar{M}_w$, $\bar{M}_n$, the dispersity index $\bar{M}_w/\bar{M}_n$ and $\bar{R}_G$ (nm) were established using ASTRA® software from Wyatt Technology Corporation (version 5.3.2.13 for PC), as previously described (Rolland-Sabaté, Amani, Dufour, Guilois, & Colonna, 2003; Rolland-Sabaté et al., 2007).

The average shrinking factor g_M ($g_M = \bar{R}^2_{GW(br)}/\bar{R}^2_{GW(lin)}$), where $\bar{R}_{GW(br)}$ and $\bar{R}_{GW(lin)}$, are the weight average radii of gyration of the branched molecule and of its linear equivalent at the same molar mass) and the apparent particle density ($d_{Gappw} = \bar{M}_w/(4\pi/3)\bar{R}^3_{GW}$) were calculated from the A4F-MALLS data, as well as the average number of branching points per macromolecule ($\bar{B}$) and the average number of glucosyl units in a linear chain per branching point ($\overline{DP}_w/\bar{B}$) as previously described (Rolland-Sabaté et al., 2007). $\bar{R}_{GW(lin)}$, was deduced from the equation linking molar mass and the radius of gyration established for strictly linear amyloses (Rolland-Sabaté, Colonna, Mendez-Montealvo, & Planchot, 2008).

The data analysis was based on a polymer science theory, the ABC three-functional polycondensation model (ABC model) proposed by Burchard (1972, 1983). The amylopectin branching characteristics were approached using the theory of hyperbranched macromolecules which are considered to arise from a polycondensation reaction of monomers containing one, so-called functional, group A and at least two other functional groups, B and C. In this statistical model, the branching points are not distributed in a random way within the macromolecule. In amylopectin, the reducing-end group establishes a focal-end group A, which due to the specificity of biosynthesis enzymes, can only react with the hydroxyl groups B and C in the C_4 and C_6 positions of the ring. A reaction with B is 25 times more frequent than with C. If both B and C groups react, a branching point is created. g_M is then given by the following relation (Burchard, 1983):

$$g_M = \frac{\bar{R}^2_{GW(br)}}{\bar{R}^2_{GW(lin)}} = \frac{4[1+2\bar{B})^{1/2}]}{[1+(1+2\bar{B})^{1/2}]^2}$$

Size distributions (hydrodynamic radius distributions) were determined using the hydrodynamic radius (R_H) versus elution time calibration curves previously determined with latex spheres in A4F (Rolland-Sabaté, Guilois, Jaillais, & Colonna, 2011).

The distribution of linear chains was determined after debranching of starch with an isoamylase as previously described (Rolland-Sabaté et al., 2012), using HPAEC-PAD as described in Section 2.2.2.

The water employed for all experiments was produced using a RiOs™5 and Synergy purification system (Millipore, Bedford, MA, USA).

Table 1
Amylose content of cassava starches.[a]

Sample name	Amylose content (%)		
	Colorimetric [b] (%)	DSC [c] (%)	IBC [d] (%)
TMS60444	16.5 (0.1)	14.4 (0.7)	16.4 (0.1)
WXA19	6.5 (0.5)	7.1 (0.4)	5.3 (3.0)
WXB8	2.2 (0.1)	3.3 (0.2)	0.0 (N.A.)
WXB9	0.7 (0.4)	0.0 (N.A.)	0.0 (N.A.)
WXB10	4.1 (1.2)	2.1 (0.1)	3.3 (1.9)
WXB13	4.2 (1.6)	2.3 (0.1)	2.8 (1.6)
WXB23	1.7 (0.4)	0.0 (N.A.)	0.0 (N.A.)
WXN	0.0 (N.A.)	0.0 (N.A.)	0.0 (N.A.)

[a] Standard deviations are given within parenthesis. N.A.: not available.
[b] Values obtained from colorimetric measurements.
[c] Values obtained from DSC measurements.
[d] Values obtained from IBC measurements.

3. Results and discussion

3.1. Amylose content

The amylose contents of studied cassava starches varied from 0% for WXN to 16.5% for TMS60444 (Table 1). These amylose contents were in line with those determined by other authors for wild type and waxy cassava starches (Gomand, Lamberts, Derde, et al., 2010; Gomand, Lamberts, Visser, & Delcour, 2010; Rolland-Sabaté et al., 2012; Sánchez et al., 2009; Tetchi, Rolland-Sabaté, Amani, & Colonna, 2007; Zhao et al., 2011). WXN, WXB8, WXB9, and WXB23 exhibited the lowest amylose content (from 0 to 2.5%) and WXA19 the highest (6.5%) amount of amylose (Table 1). The transgenic starches are therefore named also waxy clones. The values obtained using colorimetric, DSC and IBC measurements agreed detecting considerably lower amylose contents for the transgenic and natural waxy starches than TMS60444, despite some variation for particularly low-amylose transgenic waxy starches (WXB8, WXB9 and WXB23).

3.2. Starch granule size, morphology and crystallinity

The distributions were unimodal for all the cassava starches (results not shown). As shown in Table 2, the transgenic clones and their parental clone TMS60444 showed very similar average

Table 2
Average granule diameter, crystallinity and thermal properties of native starches (standard deviations are given within parenthesis).

Sample name	Average granule diameter[b] (μm)	Crystallinity[a]			Thermal properties[c]				
		Crystallinity (%)	A type (%)	B type (%)	T_o[c] (°C)	T_p[c] (°C)	T_c[c] (°C)	ΔH (J g^{-1})	ΔT (°C)
TMS60444	12.1 (2.1)	35	80	20	54.0 (1.1)	63.3 (0.9)	72.7 (1.5)	12.9 (1.3)	18.7
WXA19	12.9 (2.1)	35	80	20	55.2 (1.0)	69.3 (1.0)	77.0 (1.5)	13.9 (1.4)	21.8
WXB8	12.5 (2.1)	35	80	20	58.9 (1.2)	68.2 (0.7)	78.3 (1.6)	13.7 (1.4)	19.4
WXB9	12.7 (2.1)	35	80	20	56.8 (1.1)	64.4 (0.9)	75.5 (1.5)	15.0 (1.5)	18.8
WXB10	12.1 (2.1)	35	80	20	59.7 (1.2)	68.6 (1.0)	77.6 (1.6)	13.1 (1.3)	18.0
WXB13	12.1 (2.1)	35	75	25	56.9 (1.1)	68.0 (1.0)	77.1 (1.5)	13.2 (1.3)	20.2
WXB23	13.0 (2.1)	35	80	20	57.5 (1.2)	69.4 (1.0)	77.5 (1.6)	13.3 (1.3)	19.9
WXN	16.9 (2.0)	40	85	15	61.2 (0.4)	68.6 (0.7)	75.7 (1.9)	16.9 (1.4)	14.5

[a] Values obtained from X-ray diffraction, experimental uncertainties were 5% for A type or B type content and 3% for crystallinity. Water content 20%.
[b] Values obtained from laser diffractometry.
[c] Values obtained from DSC: T_o: onset gel temperature; T_p: peak gel temperature; T_c: conclusion temperature. Standard deviations are given within parenthesis. Water content 80%.

granule sizes (12–13 μm) and distributions of granule diameter as well whereas, the natural waxy starch exhibit a higher average granule size (16.9 μm). It can be suggested, therefore, that no change for granule size could be observed as result of the genetic modification by silencing the GBSSI expression. Even if the average granule size of these cassava clones were in the range of those generally reported for cassava starches (Ceballos et al., 2008; Charles, Chang, Ko, Sriroth, & Huang, 2005; Gomand, Lamberts, Derde, et al., 2010; Gomand, Lamberts, Visser, et al., 2010; Moorthy, 2002; Rolland-Sabaté et al., 2012; Tetchi et al., 2007), they were smaller than those reported for amylose-free potato and waxy maize starches (Gomand, Lamberts, Derde, et al., 2010; Gomand, Lamberts, Visser, et al., 2010; Rolland-Sabaté et al., 2012)

SEM (Fig. 1, left) confirmed the similarity of granule size measured with granulometry for TMS60444, WXB9 and WXB13. For parental and transgenic cassava clones, the granules were spherical and truncated and some of them shown facets. The morphologies of the granules from the transgenic waxy clones were very similar to that of their parental clone and similar to the observations reported previously on natural waxy cassava and wild type cassava starches (Rolland-Sabaté et al., 2012).

The crystallinity of native cassava starches was 35% for transgenic waxy clones and TMS60444 and 40% for natural waxy cassava (Table 2). The crystallinity of transgenic clones was systematically lower than that reported for waxy maize starches (38, 40 and 43% by Zobel (1988), Buléon, Colonna, Planchot, & Ball (1998) and Rolland-Sabaté et al. (2012), respectively) and generally lower than those reported for amylose-free potato starches (34–38.5 and 43 by Gomand, Lamberts, Derde, et al. (2010) and Rolland-Sabaté et al. (2012), respectively). The crystallinity of TMS60444 (35%) fell in the range of values reported generally for wild type cassava starches (38, 40 and 33–35% by Zobel (1988), Gomand, Lamberts, Derde, et al. (2010) and Rolland-Sabaté et al. (2012), respectively); whereas the crystallinity of transgenic clones (35%) was lower than the values previously reported for other amylose-free cassava starches (49 and 40% by Gomand, Lamberts, Derde, et al. (2010) and Rolland-Sabaté et al. (2012), respectively). No change in crystallinity was observed between TMS60444 and transgenic waxy clones in contrast to results obtained on maize (Zobel, 1988), cassava and potato, (Gomand, Lamberts, Derde, et al., 2010). The genetic modification leading to the transgenic clones therefore, did not modify crystallinity either. All cassava starches exhibited a mixture of A- and B-type crystallites with a majority of A type (75–85%), in agreement with literature data (Gomand, Lamberts, Derde, et al., 2010; Hoover, 2001; McPherson and Jane, 1999; Rolland-Sabaté et al., 2012).

3.3. Thermal properties of starches

ΔH values were between 12.9 and 16.9 J g^{-1} for TMS60444 and WXN starches respectively (Table 2). The lowest values obtained for transgenic cassava (namely 13.1, 13.2 and 13.3 J g^{-1}) correspond to WXB10, WXB13 and WXB23 starches, respectively. These values were statistically similar to that of the normal cassava starch from TMS60444 (12.9 J g^{-1}). The highest ΔH values were found in WXB9 and WXN starches (namely 15.0 and 16.9 J g^{-1}). The starch from transgenic clone WXB9 was the only one suggesting some change for ΔH may have occurred as a result of the genetic engineering. ΔH reflects the organization of double helices of amylopectin and is known to be linked to the fusion of the crystalline structure and then it increases with crystallinity (Zobel, Young, & Rocca, 1988). DSC results agreed well with crystallinity measurements as the more crystalline cassava starch (40%), WXN, exhibited the highest ΔH value, WXB9 starch made the exception. However, in literature, ΔH has been generally reported to be higher for waxy starches of maize and cassava (Gomand, Lamberts, Derde, et al., 2010; Rolland-Sabaté et al., 2012; Zobel et al., 1988). It is not the case for transgenic clones, excepted for WXB9. The high ΔH value obtained for WXB9 could then be the result of the absence of amylose in this clone.

T_p values varied from 63.3 for TMS60444 to 69.4 °C for WXB23 (Table 2). All transgenic waxy cassava starches and the natural waxy cassava starch WXN, had high T_p (68.0–69.4 °C) compared with the normal TMS60444. The only exception was WXB9, which showed a low value (64.4 °C), close to the TMS60444 one. These data were in line with the literature which reports higher T_p values for waxy starches of maize and cassava (Gomand, Lamberts, Derde, et al., 2010; Rolland-Sabaté et al., 2012), WXB9 starch being the exception. The low value of T_p obtained for WXB9 may have been due to a larger amount of crystalline defects that are known to decrease the melting temperature of crystallites (Jane, Wong, & McPherson, 1997; Jane et al., 1999). Transgenic clones and TMS60444 exhibited a higher ΔT (Table 2) compared to WXN. Among transgenic clones the broadest gelatinization peak (ΔT of 21.8 °C) was observed for WXA19, and the smallest value of ΔT (18.0 °C) was reported for WXB10.

The broad temperature range (ΔT) reveals the variety of crystalline organization and stability among the granules (Garcia,

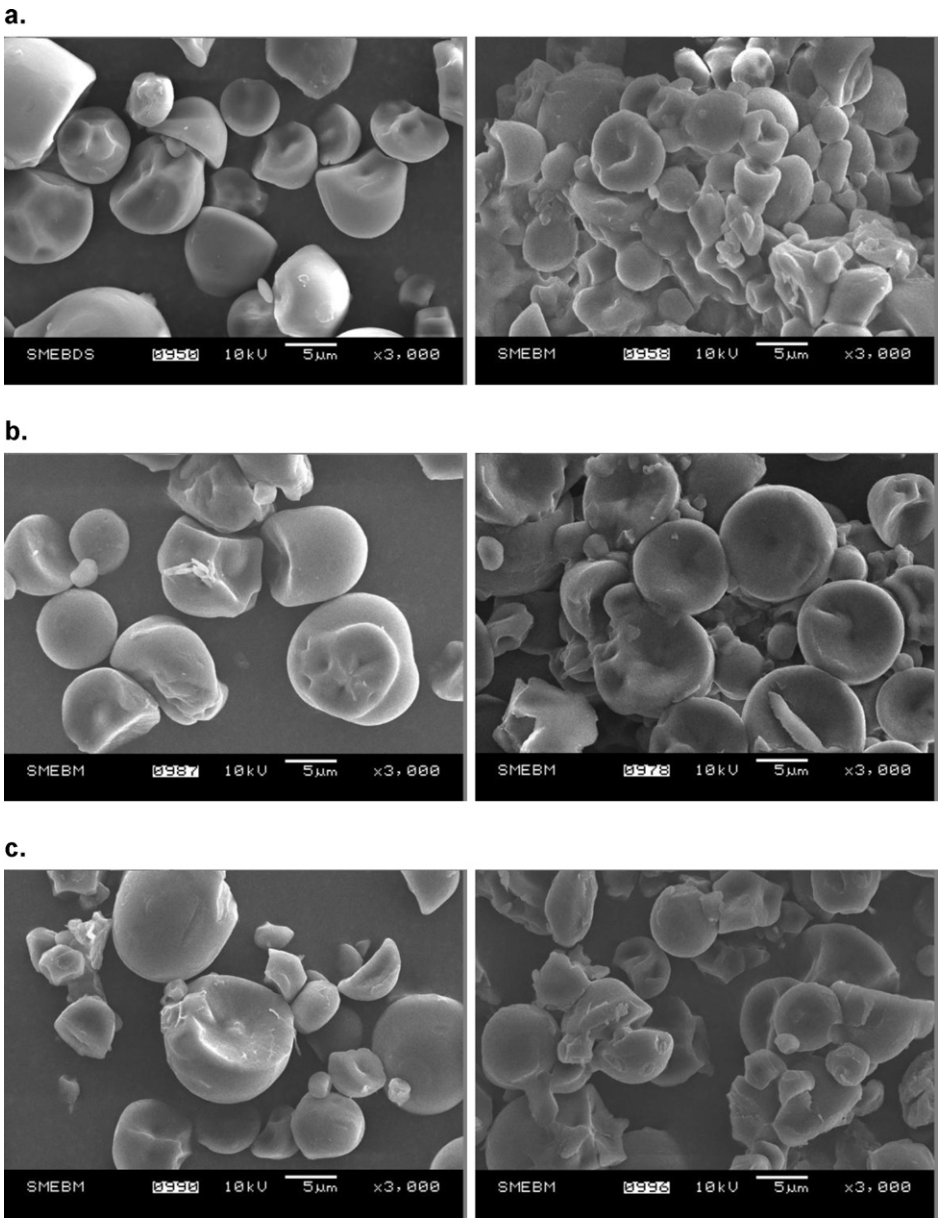

Fig. 1. Scanning electron microphotographs (3000×) of native (left) and 2-days lintnerized (right) cassava starches from parental TMS60444 (a) and transgenic clones WXB9 (b) and WXB13 (c).

Colonna, Bouchet, & Gallant, 1997; Zobel et al., 1988), i.e. the distribution of the granules structure. Then, WXN had probably a more homogeneous granule structure than transgenic and TMS60444 starches whereas WXA19 granule structures showed the largest variety, which may be related to a large amount of crystalline defects (Blennow, Bay-Smidt, Olsen, & Moller, 2000).

WXA19, WXB8, WXB9, WXB10, WXB13 and WXB23 showed similar thermal properties and a slightly higher resistance toward thermal breakdown compared with TMS60444 (higher values of T_p and ΔH). These transgenic genotypes could then have a slightly more organized structure than their parental genotype, particularly the WXB9 clone which exhibited the highest ΔH. Moreover, the thermal resistance of these transgenic waxy clones and TMS60444 is slightly lower than that for WXN (similar values of T_p, but lower T_o and ΔH), similar to the waxy maize starch one and lower than the amylose-free potato one (generally lower values of T_p, T_o and ΔH) (Gomand, Lamberts, Derde, et al., 2010; McPherson and Jane, 1999; Rolland-Sabaté et al., 2012).

3.4. Starch ultrastructure

The ultrastructure of cassava starch granules was approached by using mild acid hydrolysis (lintnerization) (Robin, Mercier, Charbonnière, & Guilbot, 1974) which is known to preferentially remove the amorphous parts of the granule. Dextrins called lintners, which correspond mainly to the crystalline residues, were produced (Biliaderis, Grant, & Vose, 1981).

As expected, mild acid hydrolysis induced an increase in crystallinity for all the cassava samples, even after only 2 days of hydrolysis (Table 3). After lintnerization process (2 days or 10 days), TMS60444 starch residues retained the same X-ray pattern whereas the B-type contribution disappeared in diffraction diagrams recorded from all other lintnerized starches, which displayed

Table 3
Lintnerized starches characteristics.

Lintnerized starches	Days of hydrolysis	Hydrolysis (%)	Crystallinity[a]				Chain distribution[b]				
			Crystallinity (%)	A type (%)	B type (%)	Water content (%)	Major group DP	Minor group DP	Max DP detected	Average DP	Dextrins of DP > 20 (%)
TMS60444	2	30	57	80	20	19	–	–	–	–	–
TMS60444	10	77	–	85	15	–	13	24/30/38	56	19.1	37.3
WXA19	10	78	53	100	0	14	13	26	43	18.6	38.7
WXB8	2	32	58	100	0	18	–	–	–	–	–
WXB8	10	80	73	100	0	16	13	26	42	18.7	39.9
WXB9	2	37	55	95	5	17	–	–	–	–	–
WXB9	10	87	69	100	0	16	13	26	42	18.6	40.2
WXB10	2	30	57	100	0	18	–	–	–	–	–
WXB10	10	83	77	100	0	17	13	26	42	18.6	39.6
WXB13	2	34	58	90	10	18	–	–	–	–	–
WXB13	10	79	–	100	0	–	13	26	42	18.7	39.6
WXB23	10	78	74	100	0	15	13	26	44	18.4	37.7
WXN	2	26	52	100	0	18	–	–	–	–	–
WXN	10	78	–	100	0	–	14	25–26	43–44	18.8	39.8

[a] Values obtained from X-ray diffraction, experimental uncertainties were 5% for A type or B type content and 3% for crystallinity.
[b] Values obtained from HPAEC-PAD, standard deviation was 3%.

a 100% A-type crystallinity after 10 days of hydrolysis (Table 3). McPherson and Jane (1999) observed similar allomorphic change from A + B-type to (pure) A-type for yam and sweet potato starches after 12 days hydrolysis and suggested that the B polymorph had preferentially hydrolyzed in these starches.

After 2 days of lintnerization, weakly hydrolyzed cassava granules could be observed by SEM. Microphotographs of TMS60444, WXB9 and WXB13 residues of starch granules after 2 days of mild acid hydrolysis showed a lot of granules' fragments, granules displaying a ghost pattern and granules with a reduced size (Fig. 1). TMS60444 and WXB9 mild acid hydrolysis residues displayed granules with softer edges and big holes on their surface area (Fig. 1a and b), whereas WXB13 residues showed jagged granules with stamped areas and "peeled orange" like zones on their surface area (Fig. 1c).

After 2 days, the solubilization extent ranged from 26% (WXN) to 37% (WXB9) (Table 3). Slightly higher hydrolysis extents were observed for transgenic waxy starches compared to TMS60444 in line with previous results obtained on waxy maize, amylose-free potato (Bertoft, 2004; Jane et al., 1997; Rolland-Sabaté et al., 2012) and legume starches (Biliaderis et al., 1981), WXB10 made the exception. On the opposite, the 26% solubilization observed for WXN showed that this starch was slightly less susceptible to lintnerization than the other cassava samples studied (30–37% solubilization). The higher granule size observed for WXN would explain partly this result.

After 10 days hydrolysis, WXB9 and WXB10 displayed the highest mild acid hydrolysis extents (83 and 87%, respectively) and TMS60444 the lowest (77%). The other cassava starches showed intermediate and similar solubilization extents (78–80%). All cassava starches residues obtained after 10 days of hydrolysis showed HPAEC-PAD profiles (Fig. 2) with two maxima: a first major peak corresponding to DP 13–14 and a second minor peak corresponding to DP 24–26, excepted for TMS60444 which displayed a shoulder at DP 17 and two additional maxima, at DP 30 and 38 (Fig. 2a). The two groups of chains corresponding to DP 13–14 and to DP 24–26 have already been reported in literature for starches subjected to mild acid hydrolysis (Bertoft, 2004; Gérard et al., 2002; Jane et al., 1997; Rolland-Sabaté et al., 2012). The first major peak (DP 12–16) was previously attributed to the linear fraction and the second maximum (DP > 20) to the single-branched fraction (Robin et al., 1974). Considering transgenic waxy cassava, the chain distributions of WXA19, WXB8, WXB10 and WXB13 lintners were strictly identical (Fig. 2b and c) whereas WXB23 lintner showed more linear (short) chains (Table 3, Fig. 2a and b) and WXB9 lintner displayed slightly less linear chains of DP 10–15 and slightly more very short chains (DP 5–9) and long chains (DP > 20) (Table 3, Fig. 2a and b). The distribution of TMS60444 lintner is comparable with data reported for normal maize (Rolland-Sabaté et al., 2012) but different from the data reported for wild type cassava (Rolland-Sabaté et al., 2012): TMS60444 exhibited less amount of long chains. The presence of amylose in TMS60444 (Table 1) would probably explain the higher amount of chains of DP > 29. These chains would then be mainly linear by analogy to Gérard et al. (2002) and Bertoft (2004) findings in the case of ae maize and potato starches, respectively. Moreover, in TMS60444 lintner the proportion of B-type crystallites was retained during mild acid hydrolysis (15–20%). The DP > 29 chains were not attacked by the acid suggesting that they were not in the amorphous phase, but probably involved in "long" double helices. Although amylopectin alone is assumed to be responsible for starch crystallinity, amylose may then be involved in crystallites, as already suggested by Gérard et al. (2002).

The chain distribution of WXN solid residues was similar to that for WXB23, except for the shoulder at DP 17 (Table 3, Fig. 2b), which was also observed for TMS60444 solid residues (Fig. 2a).

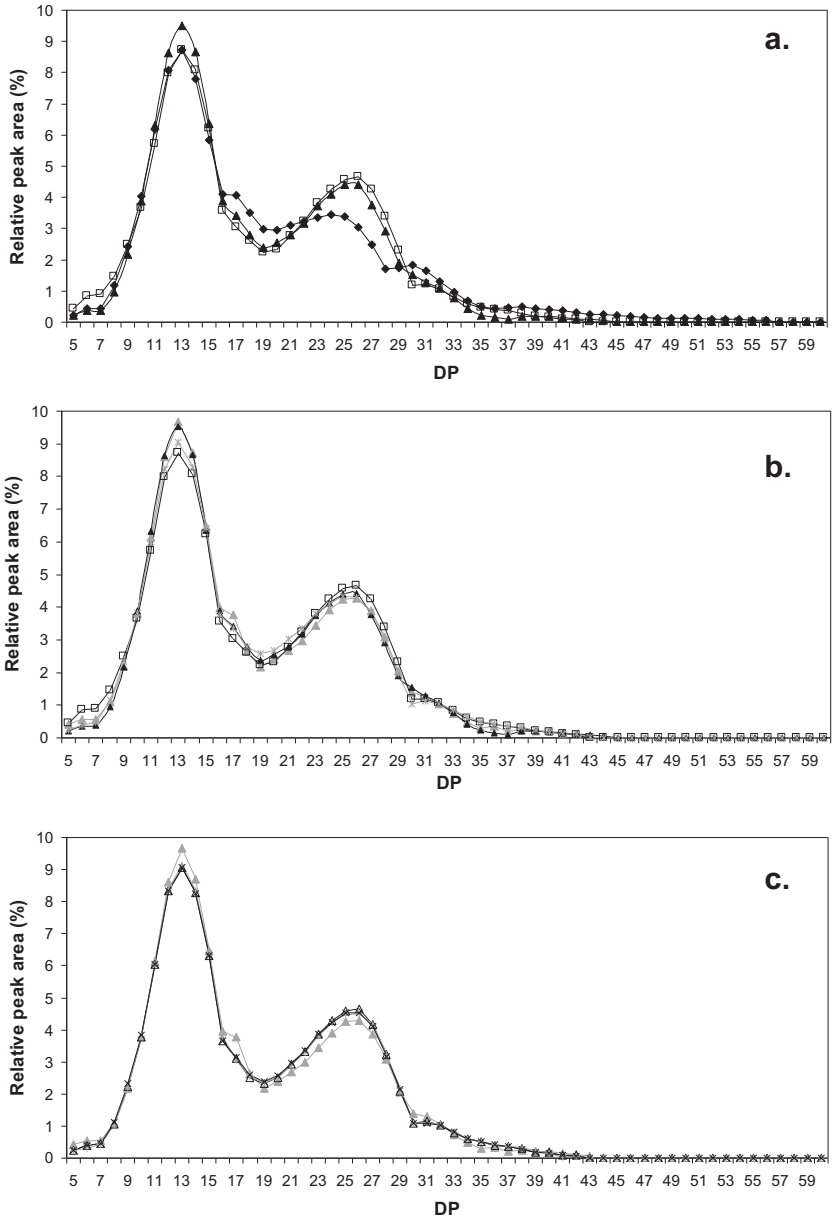

Fig. 2. Chain length distribution of 10 days lintners obtained using HPAEC-PAD. (a) TMS60444 (parental transgenic cassava) (black diamonds), WXB9 (open black squares) and WXB23 (black triangles) lintners; (b) WXA19 (gray crosses), WXB9 (open black squares), WXB23 (black triangles) and WXN (natural waxy cassava) (gray triangles) lintners and (c) WXB8 (empty black triangles), WXB10 (black crosses), WXB13 (gray plus) and WXN (gray triangles) lintners. DP: degree of polymerization.

3.5. Macromolecular characteristics of starches

3.5.1. Complexation with iodine

λ_{max} for cassava starches ranged from 528 nm (WXN) to 583 nm (TMS60444) (Table 4). WXB9 and WXB23 exhibited the lowest λ_{max} among transgenic starches (530–531 nm, respectively). The highest value (569 nm) among transgenic clones was observed in WXA19. The amylose:amylopectin ratio influences the λ_{max} values: the higher the amylose content, the higher the λ_{max} value (Tables 1 and 4). The increase of λ_{max} was indicative of longer α-(1,4) linear chains for an homogeneous media containing one type of macromolecule, i.e. it is related to the degree of polymerization between two α-(1,6) links (John, Schmidt, & Kneifel, 1983). The lowest λ_{max} observed from the strictly amylose-free cassava starches, i.e. WXN, WXB9, and WXB23 would then account for the shortest linear chain lengths that interact with iodine. In addition, these starches exhibited similar λ_{max} values, thus probably similar linear chain lengths.

3.5.2. Macromolecular features

The eight starches were injected into an A4F-MALLS system. They were solubilized with good recoveries: from 88–89% (for TMS60444, WXA19 and WXB9) to 100% (for WXB8) with an average value of 93%. Elution recoveries, i.e. the percentage of macromolecules percolated through the A4F channel were 100%. The fractionation response was then quantitative for all samples.

A4F operates a size fractionation (i.e. by hydrodynamic radius). For linear polymers, there is a direct relation between hydrodynamic radius and molar mass and radius of gyration but not for branched polymers, such as amylopectin. The radius of gyration and the molar mass distribution could not be determined for branched polymers using A4F (Gidley et al., 2010) because in this latter case,

Table 4
λ_{max} value of cassava starches and macromolecular characteristics of amylopectins determined by A4F-MALLS: weight average molar mass ($\bar{M}_w$), *z*-average radius of gyration ($\bar{R}_{Gz}$), molecular density (d_{Gappw}), hydrodynamic coefficient (ν_G) and branching parameters.[a]

Sample name	λ_{max} (nm)	A4F-MALLS analysis									
		Global parameters [b]				Branching parameters [d]					
		$\bar{M}_w$ x 10^{-6} (g mol^{-1})	$\bar{R}_{Gz}$ (nm)	d_{Gappw} [c] (g mol^{-1} nm^{-3})	ν_G	g_M	ABC model[e]	Modified ABC model Hizukuri[f]		Modified ABC model Cassava[g]	
							$\overline{DP}_w/\bar{B}$	$\overline{DP}_w/\bar{B}_{mH}$	BD_{mH} (%)	$\overline{DP}_w/\bar{B}_{mC}$	BD_{mC} (%)
TMS60444	583 (0.7)	220.0 (19.0)	211.2 (4.1)	7.6	0.43 (0.02)	0.031	173.9	20.9	4.8	19.9	5.0
WXA19	569 (6.5)	178.1 (11.2)	204.3 (2.6)	7.0	0.42 (0.02)	0.037	202.7	24.3	4.1	23.2	4.3
WXB8	533 (N.A.)	186.0 (17.0)	203.0 (1.0)	7.0	0.43 (0.02)	0.036	199.1	23.9	4.2	22.8	4.4
WXB9	530 (4.2)	252.2 (13.8)	226.6 (0.2)	6.6	0.43 (0.02)	0.032	204.9	24.6	4.1	23.4	4.3
WXB10	554 (15.2)	251.3 (7.1)	224.9 (0.3)	7.0	0.43 (0.02)	0.030	186.3	22.4	4.5	21.3	4.7
WXB13	550 (11.3)	191.0 (21.0)	203.3 (1.7)	7.4	0.43 (0.02)	0.034	185.2	22.2	4.5	21.2	4.7
WXB23	531 (0.0)	233.4 (12.5)	219.9 (1.3)	6.8	0.42 (0.02)	0.032	200.0	24.0	4.2	22.9	4.4
WXN	528 (0.0)	408.2 (62.2)	276.7 (11.1)	6.0	0.38 (0.02)	0.025	209.2	25.1	4.0	23.9	4.2

[a] Standard deviations are given within parenthesis.
[b] These values were taken over the whole amylopectin peak.
[c] $d_{Gappw} = \bar{M}_w/(4\pi/3)\bar{R}^3_{GW}$.
[d] Branching parameters: average shrinking factor ($g_M = \bar{R}^2_{GW(br)}/\bar{R}^2_{GW(lin)}$, where $\bar{R}_{GW(br)}$ is the radius of gyration of the branched molecule and $\bar{R}_{GW(lin)}$, the radius of gyration of its linear equivalent at the same molar mass. Average number of glucosyl units in a linear chain per branching point ($\overline{DP}_w/\bar{B}$) and branching degree ($BD = 100\bar{B}/\overline{DP}_w$) determined from
[e] The simple ABC model according to Burchard (1983), using the following equation: $g_M = 4\{[(1+2\bar{B})^{1/2}]/[1+(1+2\bar{B})^{1/2}]^2\}$
[f] Following the modified ABC model according to Hizukuri model where each long B chain (B2 + B3) carries on average 8.33 A and B1 chains ($\overline{DP}_w/\bar{B}_{mH} = 8.33\overline{DP}_w/\bar{B}$ and $BD_{mH} = 100\bar{B}/\overline{DP}_{wmH}$) (Hizukuri, 1986; Rolland-Sabaté et al., 2007); or
[g] Following the modified ABC model for cassava amylopectin (Laohaphatanaleart et al., 2010; Pérez and Bertoft, 2010) where each long B chain carries on average 8.75 A and B1 chains ($\overline{DP}_w/\bar{B}_{mc} = 8.75 \times \overline{DP}_w/\bar{B}$ and $BD_{mC} = 100\bar{B}/\overline{DP}_{wmC}$).

each fraction of a given size contains molecules with various molar masses and radii of gyration, i.e. different molecular structures.

Size distributions were then determined from A4F fractograms using hydrodynamic radius (R_H) versus elution volume calibration curves as previously described (Rolland-Sabaté et al., 2011) (Fig. 3). For all waxy starches, the size distributions displayed one peak at R_H ~137–148 nm corresponding to the amylopectin population. The size distribution of TMS60444 starch displayed two populations: the first peaking at R_H ~140 nm corresponds to the amylopectin fraction and the second displaying R_H < 35 nm to the amylose population. The size and molar mass distributions obtained for the waxy transgenic cassava starches were very similar to each other, as shown in Fig. 3 for WXB13 and WXB23.

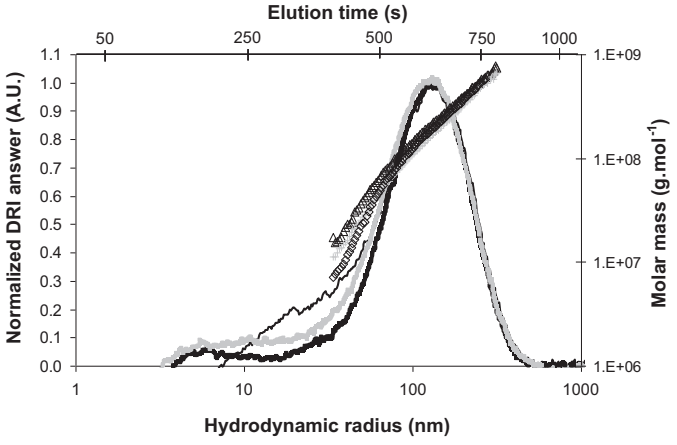

Fig. 3. Size distributions and molar masses of TMS60444 (parental transgenic waxy cassava), WXB13 and WXB23. The correspondence of elution volume and elution time to hydrodynamic radius shown on the top of the plots was made using hydrodynamic radius calibration curves according to Rolland-Sabaté et al. (2011). The normalized DRI answers were a thin black line for TMS60444 and thick gray and black lines for WXB13 and WXB23, respectively. The empty black diamonds, the gray plus and the empty black triangles represent the molar masses of TMS60444, WXB13 and WXB23, respectively.

Amylopectins displayed $\bar{M}_w$ and $\bar{R}_G$ between 178×10^6 g mol^{-1} and 408×10^6 g mol^{-1} and 203 and 277 nm, respectively (Table 4). Their dispersities, $\bar{M}_w/\bar{M}_n$, were low and of ~1.3 for all of them. These values were in line with those reported in the literature for cassava and yam starches (Pérez et al., 2011; Rolland-Sabaté et al., 2003, 2007, 2012; Tetchi et al., 2007). Transgenic cassava amylopectins exhibited similar $\bar{M}_w$ (from 178×10^6 g mol^{-1} to 252×10^6 g mol^{-1}) than their parental clone TMS60444 (220×10^6 g mol^{-1}) and lower than WXN (408×10^6 g mol^{-1}). These molar mass values were smaller than those reported for waxy maize amylopectins and higher than the ones reported for waxy potato amylopectins (Pérez et al., 2011; Rolland-Sabaté et al., 2003, 2007, 2012; Tetchi et al., 2007). Among the transgenic starches the highest $\bar{M}_w$ was obtained for WXB9, which presented one of the lowest amylose content and the smallest value was obtained for WXA19, which presented the highest amylose content (Table 4). Nevertheless, no clear relation was found between amylose content and amylopectin molar mass.

Plotting the radius of gyration versus molar mass for each fraction allows determining structural data from the exponent ν_G in the equation: $R_G = K_G M^{\nu G}$. The ν_G parameter provides information about the global conformation of macromolecules in solution. The theoretical values calculated for a sphere, a random coil in a θ solvent, a random coil in a good solvent or a rod conformation are 0.33, 0.50, 0.60 and 1.00, respectively. The ν_G values obtained for the starches analyzed in this study ranged between 0.38 and 0.43 and

were representative of a conformation between the sphere and the random coil, characteristic of branched polymers (Table 4). These values were in good agreement with data in the literature (Rolland-Sabaté et al., 2007, 2012; Tetchi et al., 2007) even if they are slightly higher for TMS60444 and its derived transgenic clones. The WXN amylopectin exhibited the lowest ν_G value suggesting that it was the more spheroidal among the analyzed starches. There were no significant differences between the ν_G values reported in Table 4 for the amylopectin of TMS60444 and its transgenic waxy derivatives, which exhibited higher ν_G values than WXN.

The determination of apparent particle density, d_{Gappw} is another way to investigate the molecule structure and conformation. Apparent particle density was calculated on the basis of a uniform density in the particle considered as a homogeneous sphere. Amylopectin d_{Gappw} ranged from 6.0 g mol^{-1} nm^{-3} for WXN to 7.6 g mol^{-1} nm^{-3} for TMS60444 (Table 4). Among transgenic waxy starches, the lowest d_{Gappw} was obtained for WXB9 and WXB23 amylopectins (6.6 and 6.8 g mol^{-1} nm^{-3}) and the highest for WXB13 amylopectin (7.4 g mol^{-1} nm^{-3}). Besides, by comparing these densities at the same molar mass (since the density increases slightly when the molar mass decreases), it could be concluded that the latter could be the densest and probably the most branched amylopectin. On the opposite, WXB9 amylopectin would be one of the least branched ones. Moreover, looking at the apparent density distributions (Supplementary data S1) it could be concluded that all the studied amylopectins exhibited very close densities and then very close branching structure.

Supplementary data associated with this article can be found, in the online version, at http://dx.doi.org/10.1016/j.carbpol.2012.10.048.

The branching characteristics of amylopectins are also reported in Table 4. The g_M values were between 0.025 for WXN and 0.037 for WXA19. Using the ABC model, $\overline{DP}_w/\bar{B}$ were determined between 173.9 for TMS60444 and 209.2 for WXN. Considering that $\bar{B}$ do not correspond to the total number of branching points of the amylopectin molecule, but only to the anchorage points of long B chains bearing A and B1 chains (Rolland-Sabaté et al., 2007) and modifying the ABC model taking into account the amylopectin structure proposed by Hizukuri (1986) (where each long B chain (B2 + B3) carries on average 8.33 A and B1 chains), the corrected average number of glucosyl units in a linear chain $\overline{DP}_w/\bar{B}_{mH}$ were determined between 20.9 for TMS60444 and 25.1 for WXN. The corrected branching degree ($BD_{mH} = 100 \times \bar{B}_{mH}/\overline{DP}_w$) ranged from 4.0 for WXN to 4.8 for TMS60444 (Table 4). TMS60444 amylopectin seemed to be the most branched. Among waxy transgenic amylopectins, WXA19 and WXB9 appeared to be the least branched, with longer chain lengths and WXB10 and WXB13 the most branched. These observations would agree with the density results. The amylopectin of the waxy transgenic varieties exhibited generally a slightly more branched structure (4.1–4.5%) than WXN amylopectin (4.0%). In the most recent model proposed for cassava amylopectin (Laohaphatanaleart, Piyachomkwan, Sriroth, & Bertoft, 2010; Pérez & Bertoft, 2010), each long B chain (B2 + B3) carries on average 8.75 A and B1 chains. Taking into account this model instead of the Hizukuri model, a corrective factor of 8.75 was applied to the data calculated using the ABC model giving corrected branching degrees (BD_{mC}) 0.2% higher than BD_{mH} (Table 4). Then, the results obtained taking into account these two different models for amylopectin structure are matchable.

Shrinking factor decreases when branching increases and decreases when molar mass increases but, in a way, depending upon the branching structure of the polymer. Shrinking factor distributions of all studied amylopectins (Supplementary data S2) were very close, thus confirming their very similar branching structure, despite the slight differences observed in terms of average branching degree.

Supplementary data associated with this article can be found, in the online version, at http://dx.doi.org/10.1016/j.carbpol.2012.10.048.

3.5.3. Branched chain length distribution

Branch chain length distributions of TMS60444, WXN, WXA19 and WXB9 amylopectins were analyzed using HPAEC-PAD. They displayed two maxima: a major peak at DP 11–12 and a minor peak at DP 43–44 (Fig. 4a and b, Table 5). The chain length distributions obtained were typical of cassava and yam starches (Jane et al., 1999; McPherson & Jane, 1999; Rolland-Sabaté et al., 2012). In general, starches from cassava had larger proportions (28.8–30.9%) of short chains (DP 6–12) and smaller proportions (8.6–9.4%) of long chains (DP > 37) compared with potato starches. They also displayed higher proportions of DP > 37, higher proportions of DP 6–12 and lower proportions of DP 13–24 than maize starches (Table 5) (Jane et al., 1999; McPherson & Jane, 1999; Rolland-Sabaté et al., 2012). Waxy and TMS60444 starches showed generally similar chain length distributions, nevertheless, slight differences were observed. The chain length distributions of the two waxy transgenic cassava (WXA19 and WXB9) were strictly the same (Fig. 4c and d, Table 5) whereas TMS60444 displayed the smallest proportions (8.6%) of long chains (DP > 37) and WXN the smallest proportions of DP 6–12 (28.8%) and the highest proportions of DP 13–24 (49.0%). The differences between TMS60444 and WXA19 and WXB9 chain length distributions (Fig. 4c) allowed to confirm (i) the very slight differences between TMS60444 and the both waxy transgenic cassava, (ii) the lower amount of long chains (DP > 34) and the higher amount of short chains (DP 9–15) in TMS60444 compared with WXA19 and WXB9. These differences in chain length distribution between the wild type and the waxy transgenic clones are in agreement with the results of Gomand, Lamberts, Derde, et al. (2010). The differences between WXN and WXA19 and WXB9 chain length distributions (Fig. 4d) confirmed the very slight differences between these three waxy cassavas in terms of DP > 37 and the lower amount of short chains (DP 6–10) in WXN compared with WXA19 and WXB9. These data are in agreement with a larger amount of crystalline defects in WXA19 and WXB9 (Jane et al., 1997, 1999). The average chain length ($\overline{CL}$) calculated from HPAEC-PAD distributions were almost identical (19.1–19.5) for the four amylopectins and in line with values reported previously for cassava and maize starches (Jane et al., 1999; McPherson & Jane, 1999; Rolland-Sabaté et al., 2012). Nevertheless, the particularly low value of highest detectable DP observed for TMS60444 (Table 5) confirmed its smaller proportion of long chains compared to waxy cassava amylopectins and could be related to a higher branching degree.

Branch chain length distributions obtained by HPAEC-PAD agreed well with the branching characteristics determined by A4F-MALLS, even if $\overline{DP}_w/\bar{B}_{HM}$ numerical values were generally higher than $\overline{CL}$ calculated from HPAEC-PAD distributions. The discrepancy between the average chain lengths determined using these both analytical techniques may be explained by a poor detection of the DP higher than 80 by HPAEC-PAD systems, which leads to an underestimation of $\overline{CL}$. Moreover, the increase of $\overline{DP}_w/\bar{B}_{HM}$ with the relative amount of DP ≥ 37 (B3 chains constitutive of the amylopectin squeleton) confirmed the effect of the internal amylopectin structure upon the branching characteristics determined by means of A4F-MALLS (Rolland-Sabaté et al., 2007).

4. General discussion

4.1. Influence of the genetic modification on the starch structure

The primary structure and the respective amounts of amylopectin and amylose macromolecules are directly linked to the

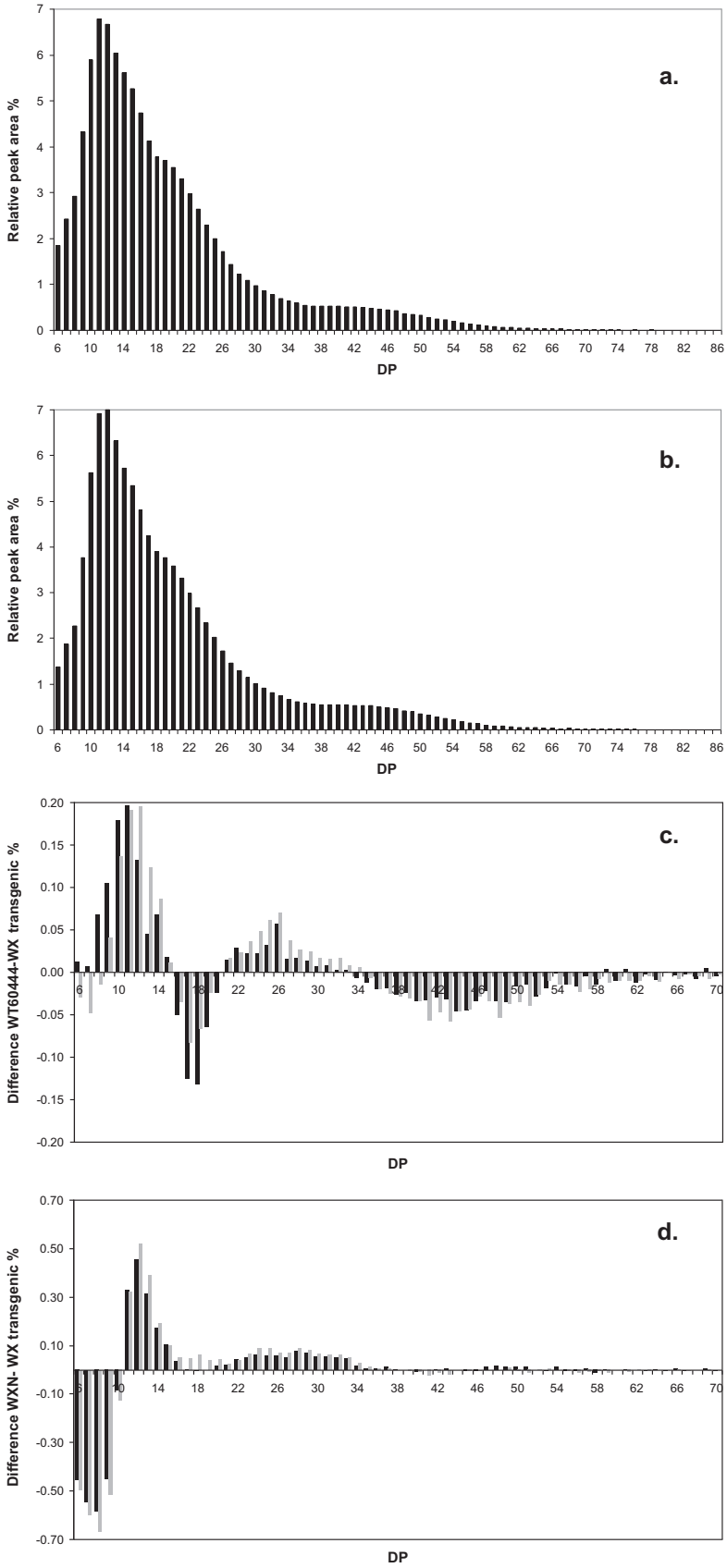

Fig. 4. Chain length distributions of TMS60444 and WXN amylopectins (a and b, respectively) and comparison of chain length distributions of WXA19 and WXB9 amylopectins presented as plots of the differences with TMS60444 (c) and WXN (d) amylopectins. The gray and the black bars correspond to WXA19 and WXB9 amylopectins, respectively.

Table 5
Chain length distributions of debranched starches obtained from HPAEC-PAD.

Type of Starch	Peak DP		% distribution					Average CL	Highest detectable DP
	I	II	DP 6–9	DP 6–12	DP 13–24	DP 25–36	DP ≥ 37		
TMS60444	11	43	11.5 (0.20)	30.9 (0.54)	48.0 (0.27)	12.5 (0.18)	8.6 (0.63)	19.1 (0.29)	79
WXA19	11	43	11.3 (0.03)	30.2 (0.01)	48.2 (0.01)	12.4 (0.08)	9.2 (0.06)	19.3 (0.02)	82
WXB9	11	43	11.6 (0.02)	30.4 (0.12)	47.9 (0.25)	12.3 (0.03)	9.4 (0.16)	19.4 (0.03)	81
WXN	12	44	9.3 (0.17)	28.8 (0.61)	49.0 (0.22)	13.0 (0.58)	9.2 (0.20)	19.5 (0.04)	83

Standard deviations are given in parenthesis.

expression of the different enzymes involved in biosynthesis (Zeeman et al., 2010). It is believed that they play a central role in starch organization, and therefore in its properties and functionalities. In particular amylose-free starches show improved performances in terms of paste clarity and stability (Jobling, 2003; Sánchez, Dufour, Moreno, & Ceballos, 2010).

Waxy cassava starches recently developed using natural mutation (Ceballos et al., 2007) and transgenesis (Zhao et al., 2011) have a significant reduction of GBSSI expression at the protein level compared to the normal cassava, especially for the WXN and WXB23 starches for which the GBSSI expression in starch is null (Ceballos et al., 2007; Zhao et al., 2011). Among waxy transgenic cassava plant clones, consistent differences in the transgene integration pattern detected by Southern blotting (Zhao et al., 2011) were observed. Single integrations were detected for WXA19, WXB10 and WXB23 whereas two copies were inserted in WXB13, WXB8 and WXB9 exhibited a single or a double integration depending upon the restriction enzyme used and they have confirmed to be the identical transgenic clones (Zhao et al., 2011).

The amount of amylose in waxy and normal cassava starches increases with the level of GBSSI in starch granules (Table 1, Ceballos et al., 2007; Zhao et al., 2011). Moreover, among waxy transgenic starches, amylose content is generally inversely proportional to the level of the GBSSI transcriptional expression and to the level of GBSSI in starch granules. Nevertheless, there are two exceptions: WXB9 which shows zero amylose content has a non negligible level of GBSSI transcriptional expression and GBSSI in starch granules, and WXB13 which displays 3–4% amylose content but a very low level of GBSSI transcriptional expression (Zhao et al., 2011). It is important to note that these two waxy clones have multiple transgene integrations, probably causing unexpected effects on targeted genes. Alternatively, the GBSSI present in WXB9 may be in an inactive form.

Molar mass and radius of gyration of waxy transgenic cassava amylopectins were in the same range as their parental clone and lower than the waxy cassava produced by self-pollination. The transgenic amylopectins displayed a very similar branching structure and showed generally a slightly more branched structure (BD_{Hm} of 4.1–4.5%; 30.2–30.4% of DP 6–12, 9.2–9.4% of DP > 37) than WXN amylopectin (BD_{Hm} of 4.0%; 28.8% of DP 6–12, 9.2–9.4% of DP > 37) but a less branched structure than their parental clone (BD_{Hm} of 4.8%; 30.9% of DP 6–12, 8.6% of DP > 37). These results confirmed that waxy mutation in cassava did not change drastically the amylopectin branching pattern, as was already observed also for maize and potato (Rolland-Sabaté et al., 2012). However, among transgenic amylopectins, the A line produced the smallest and one of the least branched amylopectins, whereas WXB10 amylopectin was one of the biggest and the most branched. No clear influence of the amylose level on the amylopectin molar mass, size and branching structure was evidenced.

The $\bar{M}_w$ and branching pattern (primary structure) of amylopectin and the amylose:amylopectin ratio control the extent and the type of crystallites formed after synthesis by the clustered short chains of amylopectin. Normal and waxy starches exhibited crystalline allomorphs proportions with mainly A-type crystallites (80%) and similar crystallinity in line with the very close branching structure of their amylopectins. However, WXN has a slightly higher crystallinity, a lower susceptibility to mild acid hydrolysis and a slightly higher resistance to thermal breakdown compared to the waxy transgenic cassava starches and their parental clone. Chains of DP 6–9 in amylopectin which are too short to built double helices produce structural defects in crystallites that decrease the crystalline lamellae density (Pérez & Bertoft, 2010). The higher amount of DP 6–9 chains in transgenic and TMS60444 starches may then explain their different behavior compared to the waxy starch obtained after spontaneous mutation. Among waxy transgenic starches, the higher mild acid hydrolysis extent and the lower T_p exhibited by WXB9 would account for a weaker crystalline structure, probably caused by defective crystals in link with the high amount of too short chains (DP 6–9) and too long chains (DP > 37) found in its amylopectin.

Surprisingly, an important variation of molar mass and thermal properties was observed for WXB8 and WXB9 which are identical transgenic clones and exhibit the same amylose content. This would mean that the molar mass and the thermal properties might be affected by other factors besides the genetic background.

Finally, the granule size and morphology was not changed in the starches having reduced amylose content by genetic modification, only with the slight differences observed in the amylopectin and crystalline structures of starches.

Surprisingly, the transgenic waxy cassava starches functional properties evaluated by RVA (Zhao et al., 2011) are not fully explained by macrostructure differences. As expected, the clones exhibiting the highest amylose content displayed the highest final viscosity after cooling. WXA19, which showed the closer RVA profile (5%) to the TMS60444 one, with a smaller viscosity, has the highest amylose content. WXB9, which has a very low amylose content, developed a higher peak viscosity compared to the natural waxy cassava starch despite a smaller granule size.

4.2. Amylopectin structure of waxy cassava starches compared to their parental one

The structure of the waxy starch obtained by spontaneous mutation is slightly different from the waxy transgenic ones. However, the structure of their parental clones is clearly different. The natural waxy and its parental cassava starch exhibit significantly different structures. Amylopectin of parental cassava starch of self-pollinated waxy clone has a smaller molar mass, a less branched structure with more long chains, the granule has a lower crystallinity and is clearly less resistant to breakdown than its waxy progeny (Rolland-Sabaté et al., 2012). On contrary only slight structure differences were found between waxy transgenic clones and their parental starch.

Acknowledgements

The authors thank S. Guilois, B. Pontoire, E. Perrin and M. De Carvalho (Research Unit on Biopolymers, Interactions and Assemblies, INRA, Nantes, France) for excellent technical support. The authors thank N. Stephant (Service commun de Microscopie à Balayage et Microanalyse (SMEBM), University of Nantes, France) for the SEM experiments. The authors acknowledge the Conseil Régional des Pays de la Loire for its financial support. This work was partially supported by grants from the National Basic Research Program (2010CB126605), the Earmarked Fund for Modern Agro-industry Technology Research System (nycytx-17) and the Sino-Swiss Science and Technology Cooperation.

References

BeMiller, J. N. (1997). Starch modification: Challenges and prospects. *Starch/Stärke*, *49*, 127–131.

Bertoft, E. (2004). Lintnerization of two amylose-free starches of A- and B-crystalline types, respectively. *Starch/Stärke*, *56*, 167–180.

Biliaderis, C. G., Grant, D. R., & Vose, J. R. (1981). Structural characterization of legume starches. 2. Studies on acid-treated starches. *Cereal Chemistry*, *58*, 502–507.

Blennow, A. (2000). Starch bioengineering. In A.-C. Eliasson (Ed.), *Starch in food* (pp. 95–127). Boca Raton, USA: CRC Press.

Blennow, A., Bay-Smidt A.M., Olsen C.E., & Moller B.L. (2000). The distribution of covalently bound phosphate in the starch granule in relation to starch crystallinity. *International Journal of Biological Macromolecules*, *27*, 211–218.

Buléon, A., Colonna, P., Planchot, V., & Ball, S. (1998). Starch granules: Structure and biosynthesis. *International Journal of Biological Macromolecules*, *23*, 85–112.

Burchard, W. (1972). Angular distribution of Rayleigh scattering from branched polycondensates. Amylopectin and glycogen types. *Macromolecules*, *5*, 604–610.

Burchard, W. (1983). Static and dynamic light scattering from branched polymers and biopolymers. *Advances in Polymer Science*, *48*, 1–124.

Ceballos, H., Sánchez, T., Morante, N., Fregene, M., Dufour, D., Smith, A. M., et al. (2007). Discovery of an amylose-free starch mutant in cassava (*Manihot esculenta* Crantz). *Journal of Agricultural and Food Chemistry*, *55*, 7469–7476.

Ceballos, H., Sánchez, T., Denyer, K., Tofiño, A. P., Rosero, E. A., Dufour, D., et al. (2008). Induction and identification of a small-granule, high-amylose mutant in cassava (*Manihot esculenta* Crantz). *Journal of Agricultural and Food Chemistry*, *56*, 7215–7222.

Charles, A. L., Chang, Y. H., Ko, W. C., Sriroth, K., & Huang, T. C. (2005). Influence of amylopectin structure and amylose content on the gelling properties of five cultivars of cassava starches. *Journal of Agriculture and Food Chemistry*, *53*, 2717–2725.

Davis, J. P., Supatcharee, N., Khandelwal, R. L., & Chibbar, R. N. (2003). Synthesis of novel starches in planta: Opportunities and challenges. *Starch/Stärke*, *55*, 107–120.

Ellis, R. P., Cochrane, M. P., Dale, M. F. B., Duffus, C. M., Lynn, A., Morrison, I. M., et al. (1998). Starch production and industrial uses. *Journal of the Science and Food Agriculture*, *77*, 289–311.

Garcia, V., Colonna, P., Bouchet, B., & Gallant, D. J. (1997). Structural changes of cassava starch granules after heating at intermediate water contents. *Starch/Stärke*, *49*, 171–179.

Gérard, C., Colonna, P., Buléon, A., & Planchot, V. (2002). Order in maize mutant starches revealed by mild acid hydrolysis. *Carbohydrate Polymers*, *48*, 131–141.

Gidley, M. J., Hanashiro, I., Hani, N. M., Hill, S. E., Huber, A., Jane, J.-L., et al. (2010). Reliable measurements of the size distributions of starch molecules in solution: Current dilemmas and recommendations. *Carbohydrate Polymers*, *79*, 255–261.

Gomand, S. V., Lamberts, L., Derde, L. J., Goesaert, H., Vandeputte, G. E., Goderis, B., et al. (2010). Structural properties and gelatinization characteristics of potato and cassava starches and mutants thereof. *Food Hydrocolloids*, *24*, 307–317.

Gomand, S. V., Lamberts, L., Visser, R. G. F., & Delcour, J. A. (2010). Physicochemical properties of potato and cassava starches and their mutants in relation to their structural properties. *Food Hydrocolloids*, *24*, 424–433.

Hizukuri, S. (1986). Polymodal distribution of the chain lengths of amylopectins, and its significance. *Carbohydrate Research*, *147*, 342–347.

Hoover, R. (2001). Composition, molecular structure, and physicochemical properties of tuber and root starches: A review. *Carbohydrate Polymers*, *45*, 253–267.

Jane, J. L., Wong, K. S., & McPherson, A. E. (1997). Branch-structure difference in starches of a- and b-type X-ray patterns revealed by their naegeli dextrins. *Carbohydrate Research*, *300*, 219–227.

Jane, J., Chen, Y. Y., Lee, L. F., McPherson, A. E., Wong, K. S., Radosavljevic, M., et al. (1999). Effects of amylopectin branch chain length and amylose content on the gelatinization and pasting properties of starch. *Cereal Chemistry*, *76*, 629–637.

Jobling, S. (2003). Improving starch for food and industrial applications. *Current Opinion in Plant Biology*, *7*, 210–218.

John, M., Schmidt, J., & Kneifel, H. (1983). Iodine–maltosaccharide complexes: Relation between chain-length and colour. *Carbohydrate Research*, *119*, 254–257.

Koehorst-van Putten, H. I. J., Sudarmonowati, E., Herman, M., Pereira-Bertram, I. J., Wolters, A. M. A., Meima, H., et al. (2012). Field testing and exploitation of genetically modified cassava with low-amylose or amylose-free starch in Indonesia. *Transgenic Research*, *21*, 39–50.

Laohaphatanaleart, K., Piyachomkwan, K., Sriroth, K., & Bertoft, E. (2010). The fine structure of cassava starch amylopectin part 1: Organization of clusters. *International Journal of Biological Macromolecules*, *47*, 317–324.

McPherson, A. E., & Jane, J. (1999). Comparison of waxy potato with other root and tuber starches. *Carbohydrate Polymers*, *40*, 57–70.

Moorthy, S. N. (2002). Physicochemical and functional properties of tropical tuber starch: A review. *Starch/Stärke*, *54*, 559–592.

Pérez, E., Gibert, O., Rolland-Sabaté, A., Jiménez, Y., Sánchez, T., Giraldo, A., et al. (2011). Physicochemical, functional and macromolecular properties of waxy yam starches discovered from "Mapuey" (*Dioscorea trifida*) genotypes in the Venezuelan Amazon. *Journal of Agricultural and Food Chemistry*, *59*, 263–273.

Pérez, S., & Bertoft, E. (2010). The molecular structures of starch components and their contribution to the architecture of starch granules: A comprehensive review. *Starch/Stärke*, *62*, 389–420.

Planchot, V., Colonna, P., & Saulnier, L. (1997). Dosage des glucides et des amylases. In B. Godon, & W. Loisel (Eds.), *Guide pratique d'analyses dans les industries des céréales* (pp. 341–398). Paris: Lavoisier.

Robin, J. P., Mercier, C., Charbonnière, R., & Guilbot, A. (1974). Lintnerized starches, gel filtration and enzymatic studies of insolubles residues from prolonges acid treatment of potato starch. *Cereal Chemistry*, *51*, 389–406.

Rolland-Sabaté, A., Amani, N. G., Dufour, D., Guilois, S., & Colonna, P. (2003). Macromolecular characteristics of ten yam (*Dioscorea* spp.) starches. *Journal of the Science of Food and Agriculture*, *83*, 927–936.

Rolland-Sabaté, A., Colonna, P., Potocki-Véronèse, G., Monsan, P., & Planchot, V. (2004). Elongation and insolubilization of α-glucans by the action of *Neisseria Polysaccharea* amylosucrase. *Journal of Cereal Science*, *40*, 17–30.

Rolland-Sabaté, A., Colonna, P., Mendez-Montealvo, M. G., & Planchot, V. (2007). Branching features of amylopectins and glycogen determined by asymmetrical flow field flow fractionation coupled with multi-angle laser light scattering (AFFFF-MALLS). *Biomacromolecules*, *8*, 2520–2532.

Rolland-Sabaté, A., Colonna, P., Mendez-Montealvo, M. G., & Planchot, V. (2008). Online determination of structural properties and observation of deviations from power law behavior. *Biomacromolecules*, *9*, 1719–1730.

Rolland-Sabaté, A., Guilois, S., Jaillais, B., & Colonna, P. (2011). Molecular size and mass distributions of native starches using complementary separation methods: Asymmetrical Flow Field Flow Fractionation (A4F) and Hydrodynamic and Size-Exclusion Chromatography (HDC-SEC). *Analytical and Bioanalytical Chemistry*, *399*, 1493–1505.

Rolland-Sabaté, A., Sánchez, T., Buléon, A., Colonna, P., Jaillais, B., Ceballos, H., et al. (2012). Structural characterization of novel cassava starches with low and high amylose contents in comparison with other commercial sources. *Food Hydrocolloids*, *27*, 161–174.

Sánchez, T., Mafla, G., Morante, N., Ceballos, H., Dufour, D., Calle, F., et al. (2009). Screening of starch quality traits in cassava (*Manihot esculenta* Crantz). *Starch/Stärke*, *61*, 12–19 (Erratum: Starch/Stärke (61) 310 (2009))

Sánchez, T., Dufour, D., Moreno, X., & Ceballos, H. (2010). Comparison of pasting and gel stabilities of waxy and normal starches from potato, maize, and rice with those of a novel waxy cassava starch under thermal, chemical, and mechanical stress. *Journal of Agricultural and Food Chemistry*, *58*, 5093–5099.

Stapleton, G. (2012). Global starch market outlook and competing starch raw materials for 732 starches by product segment and region. Cassava Starch World 2010. Centre for Management Technology (CMT). Phnom Penh, Cambodia 22–24 February.

Taggart, P. (2000). Starch as an ingredient: Manufacture and applications. In A.-C. Eliasson (Ed.), *Starch in food* (pp. 363–392). Boca Raton, USA: CRC Press.

Tetchi, F. A., Rolland-Sabaté, A., Amani, N. G., & Colonna, P. (2007). Molecular and physicochemical characterization of starches from yam, cocoyam, cassava, sweet potato and ginger produced in Ivory Coast. *Journal of the Science of Food and Agriculture*, *87*, 1906–1916.

Zeeman, S. C., Kossmann, J., & Smith, A. M. (2010). Starch: Its metabolism, evolution and biotechnological modifications in plant. *Annual Review of Plant Biology*, *61*, 209–234.

Zhang, P., Potrykus, I., & Puonti-Kaerlas, J. (2000). Efficient production of transgenic cassava using negative and positive selection. *Transgenic Research*, *9*, 405–415.

Zhao, S., Ceballos, H., Dufour, D., Sánchez, T., & Zhang, P. (2011). Development of waxy cassava with different biological and physico-chemical characteristics of starches for industrial applications. *Biotechnology & Bioengineering*, *108*, 1925–1935.

Zobel, H. F. (1988). Molecules to granules: A comprehensive starch review. *Starch-Stärke*, *40*(2), 44–55.

Zobel, H. F., Young, S. N., & Rocca, L. A. (1988). Starch gelatinization: An X-ray diffraction study. *Cereal Chemistry*, *65*, 443–446.